Optical Recognition of Atomic Steps on Surfaces

F. Baumberger,[1] Th. Herrmann,[2] A. Kara,[3] S. Stolbov,[3] N. Esser,[2] T. S. Rahman,[3] J. Osterwalder,[1] W. Richter,[2] and T. Greber[1]

[1]*Physik Institut der Universität Zürich, Winterthurerstrasse 190, CH-8057 Zürich, Switzerland*
[2]*Institut für Festkörperphysik der TU Berlin, Hardenbergstrasse 36, D-10623 Berlin, Germany*
[3]*Department of Physics, Cardwell Hall, Kansas State University, Manhattan, Kansas 66506*

(Received 3 November 2002; published 29 April 2003)

Visible and UV light spectra display striking differences in optical reflectivity for the two types of monatomic steps on copper (111) surfaces. Electronic structure calculations trace these differences to the specific contributions of $p_{\parallel}$ and $p_{\perp}$ local densities of states, parallel and perpendicular to the steps, of the distinctly coordinated corner atoms. The local origin of the spectral reflectance anisotropy is further corroborated by experiments on Cu(111) surfaces with varying step densities. Site specificity of the electronic structure of atoms in low coordinated sites on Cu(111) vicinals is thus revealed by reflectance anisotropy spectroscopy which can thereby detect step atom densities down to 10^{13} atoms/cm^2.

DOI: 10.1103/PhysRevLett.90.177402 PACS numbers: 78.40.–q, 68.37.–d, 73.20.–r, 82.45.Jn

Steps break the symmetry of surfaces which leads to a number of unique functionalities. The low coordinated atoms at steps are key players in heterogeneous catalysis [1–3], tribology [4], epitaxial growth [5], and the formation of molecular nanostructures [6]. The complex geometry of a stepped surface offers local environments of varying atomic coordination. Take, for example, steps on an otherwise flat hexagonal surface. Atoms on the flat surface have a coordination (number of nearest neighbors) of 9, while creation of a monoatomic step on this surface will produce atoms with coordination ranging from 7 to 11, depending on the orientation of the stepface. As illustrated in Fig. 1, this stepface can have either a (100) or a $(11\bar{1})$ nanofacet: the so-called *A* and *B* types of steps, respectively. The differential role of these two step types has been the subject of much discussion and debate in recent considerations of homoepitaxial growth and island shapes [7,8]. On a more general level, the question of the site selectivity for adsorption and chemical reactions has been raised [2,3]. Very recent theoretical studies [9–12] have pointed to the importance of the low coordinated sites on stepped surfaces to processes like adsorption and dissociation. What exactly makes the *A* type of stepped Cu(111) surface different from the *B* type? If local coordination plays a role, the candidate is the corner atom which has coordination of 10 on the A type and 11 on the B type.

There are a number of complementary methods for the detection of monoatomic steps on surfaces [13]. Characterization and identification of step *types* is, however, nontrivial. It requires the knowledge of the orientation of the underlying atomic lattice and the stacking sequence of the two top layers. Since the step atom density is orders of magnitudes lower than that of the surface (or bulk) atoms, it is, e.g., a formidable task to monitor step densities with video rates under conditions of high temperatures or pressures as found in gas or liquid environments. For such a task optical methods are outstanding candidates — if they are proven to recognize atomic steps. Results of experiments with visible and near UV light and related electronic structure calculations presented here respond to these challenges. They demonstrate the detection *and* differentiation of step atom densities down to the 10^{13} atoms/cm^2 range. This is accomplished with measurements of the difference in optical reflectivity for two orthogonal linear polarization components [14]. Though the diffraction limit does not allow one to produce an image of individual steps, the reflectivity *spectra* are shown to discriminate between

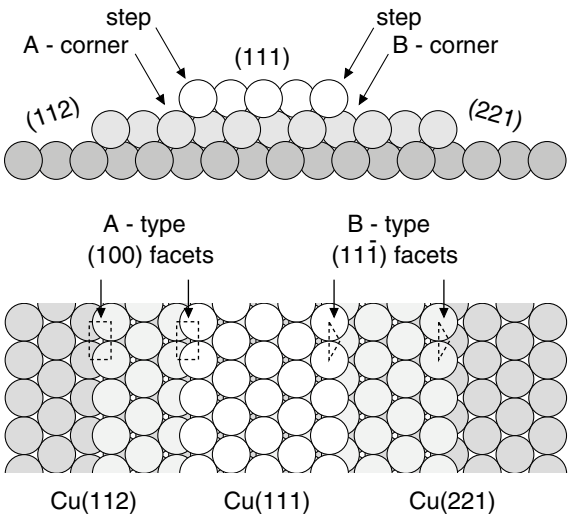

FIG. 1. Top and side view of fcc(111), the vicinal (112) (*A*-type) and (221) (*B*-type) surfaces. The two step types have either (001) or $(11\bar{1})$ nanofacets, in which the pivotal difference is the coordination number of the corner atoms of 10 and 11, respectively.

the two different step types (A and B) on vicinal hexagonally close-packed metal surfaces. Accompanying theoretical calculations trace this difference in the A- and B-type steps to the anisotropy of the partial local density of states (LDOS) of the corner atoms on the two surfaces.

Reflectance anisotropy spectroscopy (RAS) is a nondestructive, noninvasive method that has been developed by Aspnes *et al.* [14] and was put forward by the fact that the linear optical response of a cubic crystal is isotropic in the bulk, and any deviation from zero in the signal can be interpreted as a signature of the electronic structure of the surface [14]. So far RAS has been applied to semiconductors [15,16] and to metallic fcc surfaces [17–20]. This Letter reports the application of RAS to a number of vicinal surfaces of copper which, together with related *ab initio* electronic structure calculations, enables an unambiguous optical discrimination between A- and B-type steps.

The experiments were performed under ultrahigh vacuum conditions where the crystals were prepared and characterized with standard procedures that show clean surfaces with monoatomic steps [21]. Near normal RAS measurements were taken with a mobile spectrometer [22] through a low strain quartz window in the spectral range between 0.8 and 6.5 eV. The reflectance anisotropy (RA) is defined as the real part of the difference in the Fresnel reflectance amplitudes for two orthogonal directions of the light polarization, parallel and perpendicular to the steps, normalized with the mean reflectance $\mathrm{RA} = 2\mathrm{Re}[(r_{\parallel} - r_{\perp})/(r_{\parallel} + r_{\perp})]$.

Figure 1 depicts two of the investigated vicinal fcc(111) surfaces. The steps run along the close-packed $[1\bar{1}0]$ direction and their density is controlled by the miscut angle relative to the [111] direction. A-type Cu(112) has one (100) nanofacet and one terrace atom per unit cell while B-type Cu(221) has one $(11\bar{1})$ facet and two terrace atoms.

Experimental reflectance anisotropy spectra for Cu(112) and Cu(221) are shown in Fig. 2. Above 2 eV anisotropic interband transitions that determine the color of copper set in, and at 4.3 eV, both types of vicinals show a well resolved, shoulder free peak which is a maximum in the spectrum for the A type and a minimum for the B type. Thus the reflectivity along the steps at 4.3 eV is enhanced (reduced) for the A (B) type. This signature clearly discriminates the two types of surfaces.

On Cu(110) a similar RA minimum at 4.3 eV was reported [18,23,24]. This resemblance between the B-type vicinals and the (110) surface is appealing since the top layer and the second layer atoms on fcc(110) have a coordination of 7 and 11, just as the step and corner atoms on the B-type vicinals. This is to be contrasted with the distinct atomic structure and coordination of the A type: the step nanofacet presents an open (100) geometry with the step atoms still having a coordination of 7, but the corner atoms have a coordination of 10.

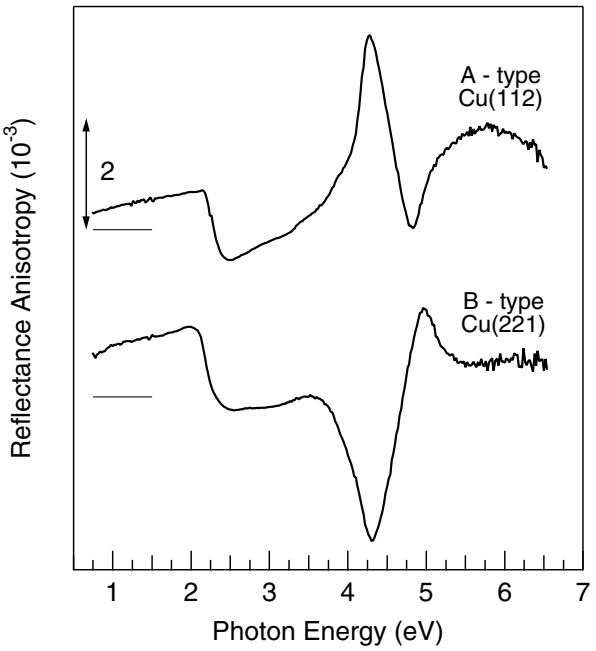

FIG. 2. Near normal reflectance anisotropy for Cu(112) and Cu(221), as a function of photon energy.

We have calculated the electronic structure of A-type Cu(112) and B-type Cu(331) with one terrace atom per unit cell using density functional theory in the local density approximation and multiple scattering theory in the framework of the local self-consistent multiple scattering method [25]. This is a local approach performed in the real space and hence it provides detailed information about the local electronic states at atomic sites with different environment. Analysis of the s, p, and d LDOS of the surface atoms reveals that the p states are most likely to be at the origin of the anisotropies of the A- and B-type vicinals observed in the spectra. Moreover, the different signs of the anisotropy at 4.3 eV can be explained by interband transitions involving the corner atom.

Optical anisotropy implies optical transitions *and* a difference in the corresponding partial LDOS of the initial and/or final states. In Fig. 3(a) the difference in the local density of p states parallel and perpendicular to the steps $p_{\parallel} - p_{\perp}$ is shown for the A- and B-type vicinals. It gives the sources of possible anisotropies in either the initial or final states of the transitions. However, not all positions in this spectrum contribute to optical transitions. In order to obtain the optical anisotropy this partial LDOS difference has to be weighted with the optical transition probability. For bulk copper a strong optical excitation at 4.3 eV is assigned to $p \rightarrow s$ interband transitions where the p derived states are located just above the d band, at a binding energy of ≈ 1 eV [26] [see the inset in Fig. 3(a)]. The calculated difference in the partial local density of states $p_{\parallel} - p_{\perp}$ for Cu(112) and Cu(331) at 1 eV indeed reflects this anisotropy in the region below the Fermi level. More strikingly, we find

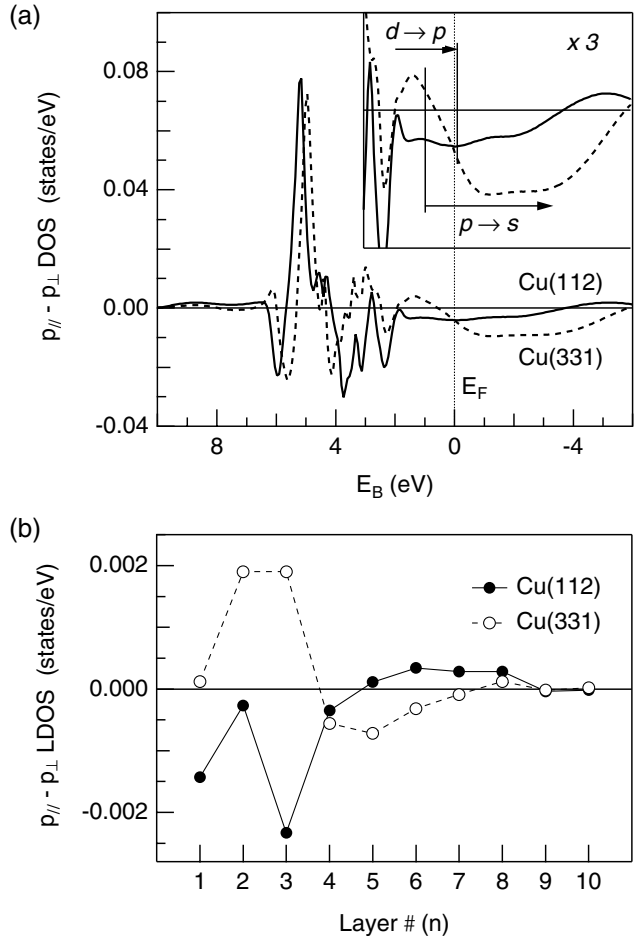

FIG. 3. (a) Total anisotropy of the partial local density of states ($p_\parallel - p_\perp$) for the top ten layers of Cu(112) and Cu(331). The inset zooms into the spectrum where the $p \rightarrow s$ (4.3 eV) and the $d \rightarrow p$ (2 eV) interband transitions occur [26]. (b) Layer resolved anisotropy of the p LDOS at a binding energy of 1 eV. The layers are numbered along the vicinal planes, starting from the outermost step atom ($n = 1$). Layer 3 corresponds to the corner atoms.

an opposite anisotropy for the A- and B-type vicinals, just as in the experimental reflectivity curves at 4.3 eV photon energy, shown in Fig. 2 and the sign of $p_\parallel - p_\perp$ agrees with the experimental reflectance anisotropy.

In order to identify the corner atoms as the main contribution to the 4.3 eV anisotropy *difference*, we plot in Fig. 3(b) the $p_\parallel - p_\perp$ LDOS, at a binding energy of ≈ 1 eV for the different layers (atoms) n on the two vicinals. Indeed, the difference in the anisotropy has its largest contribution from the corner atoms of the A- and B-type steps ($n = 3$). Figure 3(b) is also indicative of the degree of localization of the anisotropy. It decays exponentially away from the corner atoms and the screening length is of the order of the Fermi wavelength (4.6 Å for copper).

The assignment to a local origin (corner atoms) of the 4.3 eV reflectance anisotropy is further corroborated by the analysis of Cu(332) and Cu(443), i.e., two more B-type surfaces with different step densities. Figure 4 shows that the anisotropy of the peak at 4.3 eV is roughly proportional to the step density $1/\ell$, where ℓ is the step separation length. The proportionality factor α is about $-7.5 \pm 0.8 \times 10^{-3}\ell_o$, where ℓ_o^3 is the atomic volume. With a penetration depth of $80\ell_o$ for 4.3 eV photons into copper we see that the observed anisotropy may have a local origin, i.e., have its source in single atomic objects on the surface. The proportionality factor α for the measured A type has opposite sign, though the same order of magnitude. The sensitivity for the reflection anisotropy in the current setup is estimated to $\approx 0.5 \times 10^{-3}$ [27] and translates for a given orientation on vicinal copper into a step density $1/\ell$ of $\approx 10^6$ steps/cm or a step atom density $1/\ell\ell_o$ of $\approx 5 \times 10^{13}$ step atoms/cm^2.

Besides the previously discussed 4.3 eV feature, the reflectance anisotropy spectra contain a signature at ≈ 2 eV which does not change sign between A- and B-type vicinals but is in intensity proportional to the step density, too. In contrast to Cu(110) where at this energy a resonance of the highly anisotropic Shockley surface state with an unoccupied surface state occurs [18], no influence of the Shockley surface state was found. Experiments where the surfaces were exposed to oxygen and ambient air showed the reflectance anisotropy spectra to be susceptible to oxidation, though in the whole observed photon energy range no spectral feature could be assigned to the disappearance of the Shockley surface state. However, distinct signatures from the A and B types that reconstruct differently under oxygen exposure [28,29] persist and give further evidence for the usefulness of RAS. If, however, the above theoretical analysis is performed for optical excitations at ≈ 2 eV, i.e., the $d \rightarrow p$ transitions, we find in this case the step atoms ($n = 1$) to contribute the main anisotropy in the relevant unoccupied p states above the Fermi level [26]. The anisotropies have the same sign and magnitude for A and B types and are in line with the same coordination for A- and B-type step atoms [30].

From the trace back of the optical anisotropies to differently coordinated atoms we conjecture that such step signatures should be generally found on stepped surfaces. On a given vicinal fcc(111) surface the two different anisotropies from the corner and the step atoms provide the unique opportunity to determine the *nature, orientation,* and *concentration* of steps by recording reflectance anisotropy spectra for different azimuthal angles of the polarization planes of the incoming light.

In summary it is shown that RAS provides information from which it is possible to recognize very low densities of differently coordinated atoms on surfaces. Furthermore, *ab initio* electronic structure calculations are able to identify the local characteristics that distinguish the atoms in low coordinated sites on stepped surfaces. These results open the way for detailed

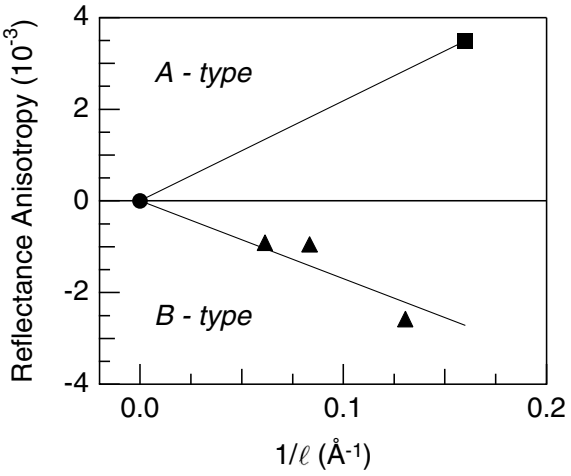

FIG. 4. Reflectance anisotropy at 4.3 eV for Cu(112) (square), Cu(111) (circle), and Cu(443), Cu(332), and Cu(221) (triangles) as a function of the step density $1/\ell$, where ℓ is the step-step separation.

investigations of site selectivity in various physical and chemical processes on heterogeneous surfaces. The findings also provide the opportunity for the exploitation of this effect in optical microscopes with spectral discrimination. Applications, such as the online control of the microscopic roughness in epitaxy or its correlation with catalytic activity can be realized.

This work has been supported by the Swiss National Science Foundation and the SFB 290 of the Deutsche Forschungsgemeinschaft (DFG). A. K., S. S., and T. S. R are supported by the U.S. Basic Energy Research Division, Department of Energy, Grant No. DE-FG03-97ER45650. A. K. thanks his colleagues at the University of Zürich for their warm hospitality. Fruitful discussions with Ph. Hofmann and L. Mochan are gratefully acknowledged.

[1] G. A. Somorjai, *Surface Chemistry and Catalysis* (Wiley & Sons, New York, 1994).
[2] T. Zambelli, J. Wintterlin, J. Trost, and G. Ertl, Science **273**, 1688 (1996).
[3] L. M. Falicov and G. A. Somorjai, Proc. Natl. Acad. Sci. U.S.A. **82**, 2207 (1985).
[4] B. N. J. Persson, *Sliding Friction: Physical Principles and Applications* (Springer, Berlin, Heidelberg, 1998).
[5] A. Zangwill, *Physics at Surfaces* (Cambridge University Press, Cambridge, 1988).
[6] R. Fasel, A. Cossy, K. H. Ernst, F. Baumberger, T. Greber, and J. Osterwalder, J. Chem. Phys. **115**, 1020 (2001).
[7] T. Michely, M. Hohage, M. Bott, and G. Comsa, Phys. Rev. Lett. **70**, 3943 (1993).
[8] C. Steimer, M. Giesen, L. Verheij, and H. Ibach, Phys. Rev. B **64**, 085416 (2001).
[9] B. Hammer and J. K. Nørskov, Phys. Rev. Lett. **79**, 4441 (1997).
[10] B. Hammer, Phys. Rev. Lett. **83**, 3681 (1999).
[11] P. Gambardella, Z. Sljivancanin, B. Hammer, M. Blanc, K. Kuhnke, and K. Kern, Phys. Rev. Lett. **87**, 056103 (2001).
[12] I. Makkonen, P. Salo, M. Alatalo, and T. S. Rahman, Phys. Rev. B (to be published).
[13] H.-C. Jeong and E. D. Williams, Surf. Sci. Rep. **34**, 175 (1999), and references therein.
[14] D. E. Aspnes, J. P. Harbison, A. A. Studna, and L. T. Florez, J. Vac. Sci. Technol. A **6**, 1327 (1988).
[15] I. Kamiya, D. E. Aspnes, H. Tanaka, L. T. Florez, J. P. Harbison, and R. Bhat, Phys. Rev. Lett. **68**, 627 (1992).
[16] A. I. Shkrebtii, N. Esser, W. Richter, W. G. Schmidt, F. Bechstedt, B. O. Fimland, A. Kley, and R. Del Sole, Phys. Rev. Lett. **81**, 721 (1998).
[17] Y. Borensztein, W. L. Mochan, J. Tarriba, R. G. Barrera, and A. Tadjeddine, Phys. Rev. Lett. **71**, 2334 (1993).
[18] Ph. Hofmann, K. C. Rose, V. Fernandez, A. M. Bradshaw, and W. Richter, Phys. Rev. Lett. **75**, 2039 (1995).
[19] A. Borg, O. Hunderi, W. Richter, J. Rumberg, and H. J. Venvik, Phys. Status Solidi (a) **152**, 77 (1995).
[20] V. Mazine and Y. Borensztein, Phys. Rev. Lett. **88**, 147403 (2002).
[21] F. Baumberger, T. Greber, and J. Osterwalder, Phys. Rev. B **64**, 195411 (2001).
[22] W. Richter and J.-T. Zettler, Appl. Surf. Sci.. **101**, 465 (1996).
[23] K. Stahrenberg, Th. Herrmann, N. Esser, and W. Richter, Phys. Rev. B **61**, 3043 (2000).
[24] J.-K. Hansen, J. Bremer, and O. Hunderi, Surf. Sci. **418**, L58 (1998).
[25] Y. Wang, G. M. Stocks, W. A. Shelton, D. M. C. Nicholson, Z. Szotek, and W. M. Temmerman, Phys. Rev. Lett. **75**, 2867 (1995).
[26] K. Stahrenberg, Th. Herrmann, K. Wilmers, N. Esser, W. Richter, and M. J. G. Lee, Phys. Rev. B **64**, 115111 (2001).
[27] This estimate for the sensitivity is taken from the scatter of the data around the α/ℓ line for the four individual *B*-type samples (see Fig. 4). From the data in Fig. 2 it can be seen that the RA signal from a given surface may be measured with a much higher accuracy. Therefore on a given sample significant RA changes in the 10^{-4} range may be detected.
[28] G. Witte, J. Braun, D. Nowack, L. Bartels, B. Neu, and G. Meyer, Phys. Rev. B **58**, 13 224 (1998).
[29] S. Vollmer, A. Birkner, S. Lukas, G. Witte, and Ch. Wöll, Appl. Phys. Lett. **76**, 2686 (2000).
[30] A. Kara *et al.* (to be published).